DOI: 10.1002/anie.201410684

Gas-Separation Membranes Loaded with Porous Aromatic Frameworks that Improve with Age**

Cher Hon Lau, Kristina Konstas, Aaron W. Thornton, Amelia C. Y. Liu, Stephen Mudie, Danielle F. Kennedy, Shaun C. Howard, Anita J. Hill, and Matthew R. Hill**

Abstract: *Porosity loss, also known as physical aging, in glassy polymers hampers their long term use in gas separations. Unprecedented interactions of porous aromatic frameworks (PAFs) with these polymers offer the potential to control and exploit physical aging for drastically enhanced separation efficiency. PAF-1 is used in the archetypal polymer of intrinsic microporosity (PIM), PIM-1, to achieve three significant outcomes. 1) hydrogen permeability is drastically enhanced by 375 % to 5500 Barrer. 2) Physical aging is controlled causing the selectivity for* H_2 *over* N_2 *to increase from 4.5 to 13 over 400 days of aging. 3) The improvement with age of the membrane is exploited to recover up to 98 % of* H_2 *from gas mixtures with* N_2*. This process is critical for the use of ammonia as a* H_2 *storage medium. The tethering of polymer side chains within PAF-1 pores is responsible for maintaining* H_2 *transport pathways, whilst the larger* N_2 *pathways gradually collapse.*

Physical aging occurs in polymers not in thermodynamic equilibrium below their glass transition temperature (T_g).[1] During aging, polymer chains converge as they attempt to achieve equilibrium and the dynamic void spaces collapse.[2] This is particularly prevalent in polymers with intrinsic microporosity (PIMs).[3] The non-linear backbone of PIM-1, contains twisted or bent spirobisindane and dibenzodioxane linkages.[4] The frustrated packing of these contorted polymer chains yields exceptionally high fractional free volume (FFV) content. However, the high FFV of PIM-1 tends to be short-lived, soon collapsing to leave fewer transport pathways. Consequently, gas permeability significantly slows,[5] but selectivity for one gas over another increases, in line with the trade-off relationship described by Robeson.[6] Reported applications of PIM-1[7] utilize this high initial FFV content.

Efforts to stop physical aging in PIM-1 typically reduce gas permeabilities, and are generalized into polymer chain rigidification[8] or FFV enhancement related methods.[9] PIM-1 is useful for high-speed gas separations with reasonable gas selectivity.[10]

Interest has recently turned to ammonia's utility as part of the H_2 economy through the efficient cracking of ammonia into its constituent of H_2 and N_2.[11] For this process to be viable, H_2 must then be efficiently isolated. Separating H_2 from N_2 can be performed at high temperatures with inorganic membranes, but this process can be problematic given the potential for ammonia present to poison the membrane.[12] Polymeric membranes are attractive in this setting given their processability at scale and comparative low cost.[13] Although PIMs are ideal for such H_2/N_2 separations,[14] they continue to suffer from physical aging.[15] Hence, this tantalizing gas-transport behavior does not persist for a meaningful time period, and is difficult to exploit.

We recently showed that the regular carbonaceous pores within a porous aromatic framework (PAF), PAF-1, can harbor side chains from super glassy polymers, and stop aging for CO_2 gas transport, whilst concomitantly tripling the permeability.[16] PAFs are tetrahedrally arranged aromatic rings self-assembled by the Yamamoto self-coupling reaction of tetrabromophenylmethane monomers.[17] Surface areas of PAFs can reach up to 5400 $m^2 g^{-1}$, and are tunable.[18]

Herein we report that PIM-1/PAF-1 membranes show selective aging for some gas mixtures that remarkably improve in selectivity over time without permeability loss for small gases (Figure 1 and Supporting Information). Analyses reveal that detailed chemical interactions propping open the transport pathways are responsible for this phenomenon. This unexpected property is exploited for gas separations relevant to ammonia cracking. The membranes show utility in efficiently isolating H_2 from N_2 without the need for high temperatures.

In our hands, H_2 and N_2 permeabilities of PIM-1 membranes stored in ambient conditions between periodic tests decrease by approximately 90 % with aging over 400 days, in line with other reports.[19] These membranes were not soaked in methanol prior to characterization. Incorporation of 10 wt % PAF-1 particles into PIM-1 enhanced the H_2 and N_2 permeabilities by 375 %, and 450 % respectively (Figure 2). There are three distinctive pore size distributions in PAF-1 centered at 5, 12, and 48 Å.[16] The 48 Å pores disappear

---

[*] Dr. C. H. Lau, Dr. K. Konstas, Dr. A. W. Thornton, Dr. D. F. Kennedy, Dr. S. C. Howard, Dr. A. J. Hill, Dr. M. R. Hill
CSIRO
Bag 10, Clayton South 3169, VIC (Australia)
E-mail: Cherhon.Lau@csiro.au
Matthew.Hill@csiro.au

Dr. A. C. Y. Liu
Monash Centre for Electron Microscopy, School of Physics
Monash University, Clayton 3800, VIC (Australia)

Dr. S. Mudie
Australian Synchrotron
800 Blackburn Road, Clayton 3168, VIC (Australia)

[**] Parts of this work were supported by the Science and Industry Endowment Fund. M.R.H. and A.J.H. acknowledge the CSIRO OCE, Dr. Detlev Fritsch, Dr. Roger Mulder, Dr. Jisheng Ma, Dr. Russell Varley, and Cameron Way for characterization advice. Parts of this work were conducted at the Australian Synchrotron, Melbourne, Victoria.

Supporting information for this article is available on the WWW under http://dx.doi.org/10.1002/anie.201410684.

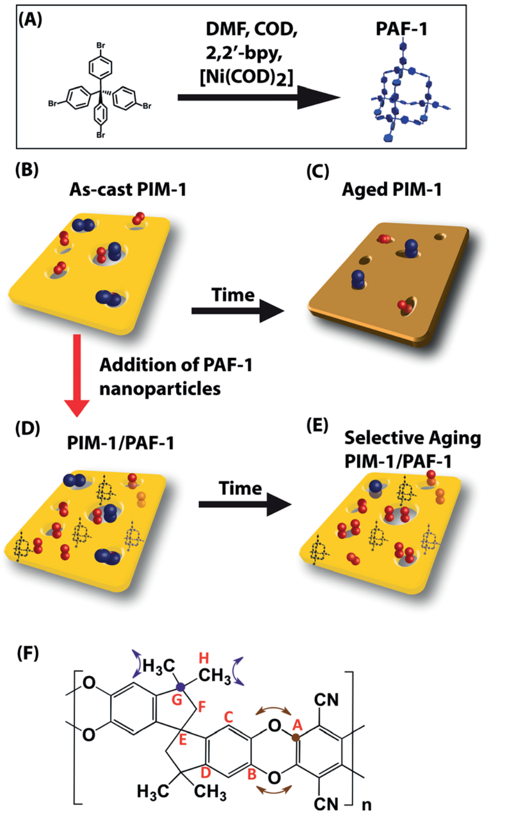

Figure 1. A) PAF-1 synthesis (COD = 1,5-cyclooctadiene). B) As-cast PIM-1 membranes, C) membranes age over time and gas permeabilities decrease as FFV content is reduced. D) Incorporating PAF-1 nanoparticles into PIM-1 yields a PIM-1/PAF-1 composite membrane and over time produces a selective aging membrane (E) that preferentially transports H_2 (red spheres) over N_2 (blue spheres). F) Structural formula of PIM-1.

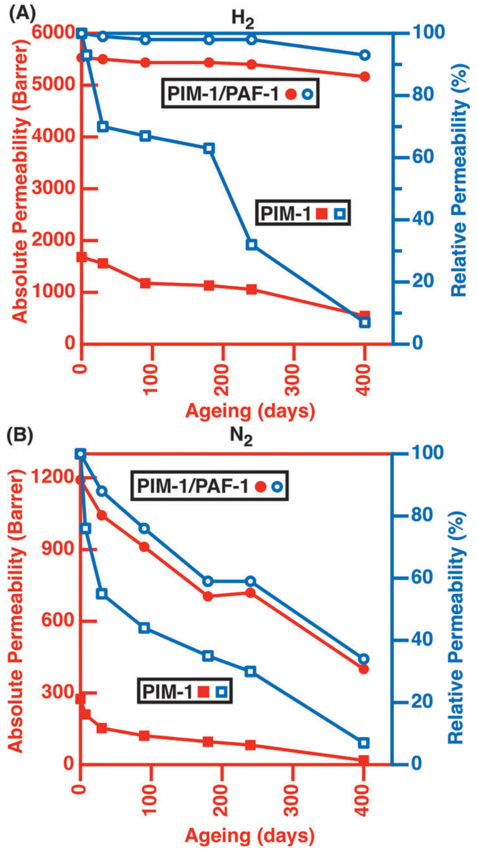

Figure 2. Absolute (red) and relative (blue) permeabilities of PIM-1 (squares) and PIM-1/PAF-1 (circles) to A) H_2, and B) N_2 as functions of time. Lines are drawn to guide the eye. Deviation of gas permeability measurements are within ±10%.

upon PAF-1 distribution in the polymer matrix, while the 5 and 12 Å pores provide additional gas sorption sites and diffusion channels. More importantly, incorporating PAF-1 into PIM-1 maintained the relative H_2 permeability at approximately 100% over 400 days, whilst relative N_2 permeability is reduced to just 10% of the original. This result stands apart from typical aging in PIM-1 membranes where all gas permeabilities decrease.[20] PAF-1 particles benefit diffusion-dominated transport of small gas molecules. The increase in initial gas permeability in PIM-1/PAF-1 aligns with the increased free volume delivered by over 5000 $m^2 g^{-1}$ of PAF-1 surface area, the number of gas transport pathways is substantially increased with its inclusion, correlating well with other porous additives in polymer membranes.[21]

Elucidation of the selective aging mechanism required an integrated series of characterization tests. Bulky moieties of PIM-1 are intercalated within PAF-1 pores owing to its favorable surface chemistry, allowing smaller polymer-free-volume elements to remain open, while larger ones collapse with physical aging. This phenomenon ensures transport pathways for smaller molecules, such as H_2 remain available, while those for the larger molecules, such as N_2, diminish with time.

Small-angle X-ray scattering (SAXS) and wide-angle X-ray scattering (WAXS) revealed pore architecture effects (Figure 3). SAXS peaks at low *q* (small pores) and high *q* ranges (large pores) detected in our membranes agree with previous results reported from multiple techniques.[19,22] PIM-1 pore size distributions obtained from SAXS/WAXS differ from those obtained using cryogenic physisorption methods,[3b] and can be attributed to the difference in detection probes. SAXS deploys X-rays which are able to determine pores as small as 0.5 Å, however cryogenic physisorption uses N_2 molecules which are unable to probe pores smaller than 3.6 Å. In PIM-1 control, peaks between $q = 0.5$ to 0.7 $Å^{-1}$ are correlated to chain-to-chain distance (P_{CC}), and are sensitive to aging; while peaks between $q = 0.8$ to 1.3 $Å^{-1}$ are attributed to the real space between inefficiently packed, kinked polymer chains, for example, the empty voids around the bulky chemical moieties (P_{RS}).[20] Aging in PIM-1 shifted the P_{CC} peak position from 0.57 $Å^{-1}$ ($d = 11$ Å) to 0.66 $Å^{-1}$ ($d = 9.5$ Å), indicating a 14% decrease in chain to chain space. The four peaks (P1–P4) between $q = 0.8$ to 2.5 $Å^{-1}$ have a distribution similar to that observed in positron analysis.[16] Aging in PIM-1 also shifted the P1, P2, and P3 peaks to higher *q* values while reducing the area under these peaks: This change corresponds to smaller pore sizes and lower pore concentration that consequently reduce H_2 and N_2 permeabilities in aged PIM-1.

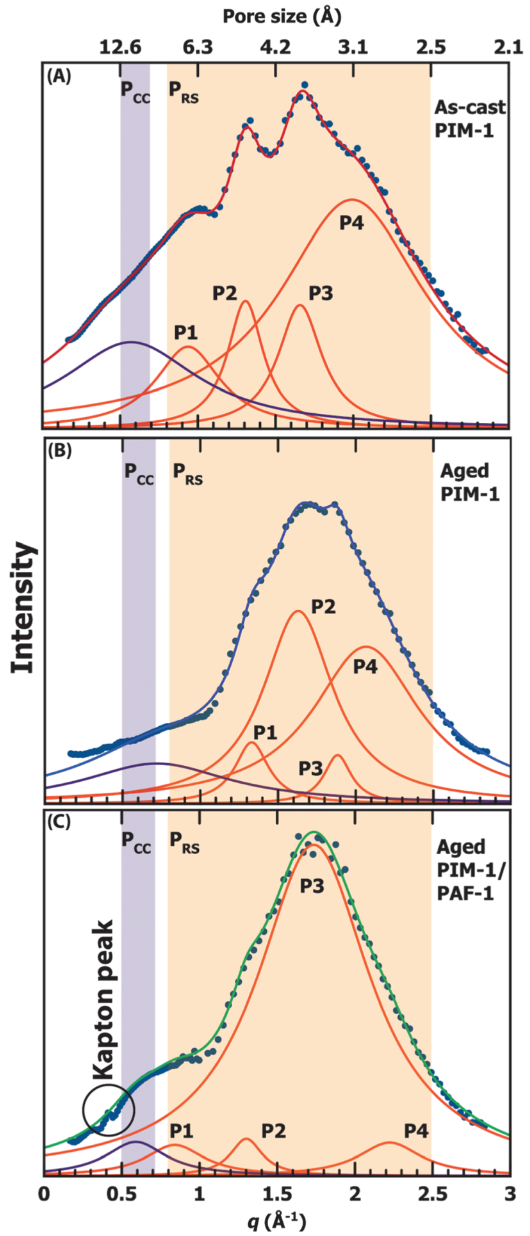

Figure 3. SAXS and WAXS of A) as-cast and B) aged PIM-1, and C) aged PIM-1/PAF-1 films. Raw data (circles) were deconvoluted to obtain P_{CC}: peaks corresponding to chain-to-chain distance, and P_{RS}: peaks correlated to real spaces between inefficiently packed polymer chains. The sharp peak in the SAXS region of aged PIM-1/PAF-1 is attributed to the signature peak of the Kapton well used during SAXS/WAXS experiments (Supporting Information).

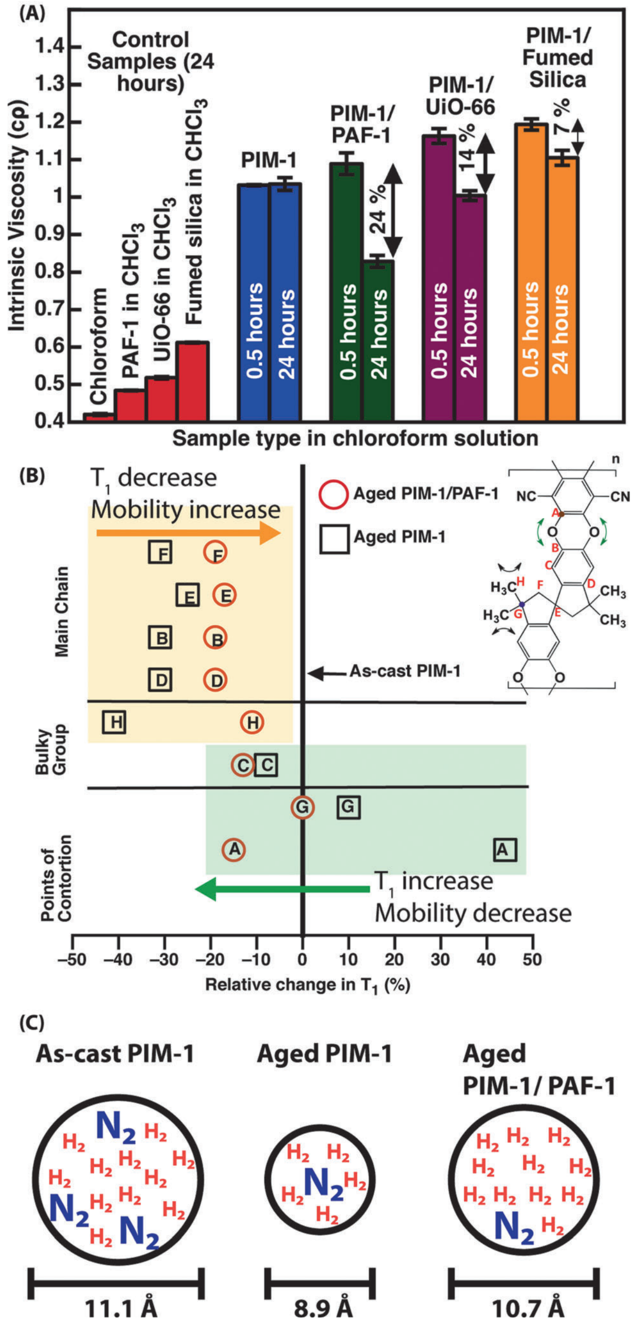

Figure 4. A) Intrinsic viscosity measurements of 10 wt% nanoparticle solutions and PIM-1/nanoparticle (10 wt% with respect to PIM-1 concentration) solutions stirred for 0.5 and 24 h. B) Relative changes of relaxation times T_1 of aged PIM-1 and PIM-1/PAF-1 films with respect to as-cast PIM-1 (set as 0%) determined by ^{13}C solid state MAS NMR spectrometry. C) Schematic representation showing that H_2 permeability in aged PIM-1/PAF-1 resembles that of as-cast PIM-1 while N_2 permeability is similar to aged PIM-1 that is, selective aging properties.

PAF-1 particles maintain pore sizes in aged PIM-1/PAF-1 sufficient for H_2 Knudsen diffusion, even after 400 days. However, PAF-1 did not stop the area reduction for all pores, which accounts for the drastic permeability losses for larger molecules, such as N_2.

Experiments were performed to directly detect the interaction between PIM-1 and PAF-1 (Figure 4 A). A control series of viscosity measurements on PIM-1 nano-additive composites was undertaken using non-porous fumed silica (FS), UiO-66 which is a Zr-based porous metal–organic framework (MOF), and PAF-1. The controls isolated the non-Newtonian behavior delivered by PIM-1 chains threading into PAF-1. Three effects can deliver this behavior (Table S1): 1) surface adsorption of polymer chains on the additive decreasing entanglement[23] (FS, UiO-66, PAF-1), 2) extra free-volume being introduced,[24] and 3) polymer chains threading into the additive's pores[25] (PAF-1). Viscosity drops of 7 % (FS), 14 % (UiO-66), and 24 % (PAF-1) align well with 1, 2, or 3 of the available mechanisms being active (Figure 4 A). Furthermore, the viscosity measurements agree with the measured gas transport properties—UiO-66 showed no selective-aging effect,[16] FS accelerated aging,[21] and our systems do not age selectively without 24 h mixing prior to casting.

The specific molecular nature of PIM-1/PAF-1 interactions was further elucidated using ^{13}C solid-state NMR (Figure 4 B). T_1 relaxation times relate to mobility levels of a specific moiety within the polymer, and are sensitive to aging in the presence of PAF-1. Carbon atoms in PIM-1 are categorized,[4a] into contortion points where PIM-1 is allowed to bend and flex, bulky chemical moieties (CN) and dimethyl (labeled H in Figure 4 B) groups, and main-chain carbon atoms, which can flex. During aging, bulky moieties drive the convergence of main chains.[26] In agreement with this situation, the mobility of the groups labeled H in aged PIM-1 is enhanced. Peak overlap precluded identifying similar findings for the CN groups, although it is likely to be present.

In comparison, PAF-1 immobilizes the centers (G) and (H) in PIM-1/PAF-1; pinpointing the interaction to bulky dimethyl groups of PIM-1 interacting with PAF-1. Reduced mobilities of main-chain carbon atoms indicate PIM-1 rigidification in PIM-1/PAF-1. The increased mobility of the centers (A) also indicates that the cyano groups of the PIM-1 chain remain mobile. This combination of fixed and mobile conformations maintains the enhanced transport of smaller H_2 molecules while the transport of larger N_2 molecules is drastically reduced over 400 days (Figure 4 C).

Key characteristics of PIM-1/PAF-1 aging were modelled alongside experimental data on the upper bound (Figure 5).[6] Remarkably, the membrane continually improves in its H_2/N_2 selectivity whilst maintaining H_2 permeability. It rivals fresh membranes which, although handling and treatment of PIM-1 has been optimized, remain prone to aging.[3,9,27] This model also confirmed that the dominant H_2 diffusion mechanism in these membranes is Knüdsen diffusion.[28] Using only the larger pore sizes from P_{CC} in Figure 3 to model polymer aging and H_2 permeability in PIM-1/PAF-1, a close match between experimental data and theoretical predictions indicates that pore size maintenance plays a dominant role in H_2/N_2 separations. Pristine PIM-1 follows an often observed aging trend with permeability loss and a slight gain in selectivity during aging, while the PIM-1/PAF-1 mixed-matrix membrane gains selectivity with no loss in H_2 permeability by decreasing N_2 permeability, thereby continually improving the H_2/N_2 selectivity.

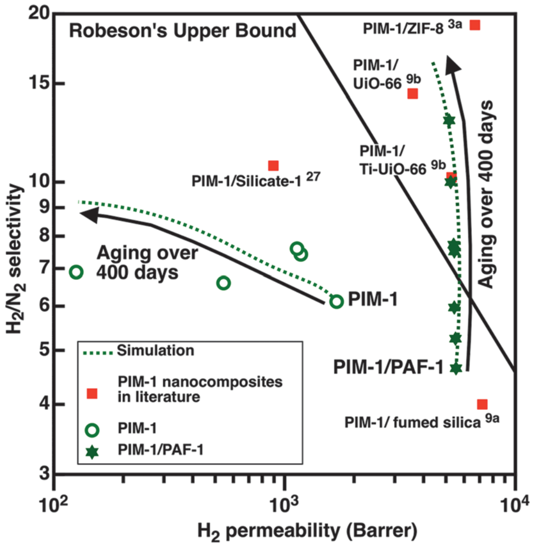

Figure 5. Comparison of H_2/N_2 separation performances of PIM-1 and PIM-1/PAF films with other reported PIM-1-based mixed-matrix membranes.[3a,9,27] plotted on Robeson's 2008 upper bound.[6]

The H_2/N_2 separation capabilities of PIM-1/PAF-1 membranes make them suitable for H_2 recovery from N_2 as found in ammonia cracking. To confirm the applicability of this unprecedented gas-transport behavior, we performed mixed-gas experiments emulating likely cracking conditions (Figure 6). As N_2 concentration increases from 50 to 70 vol %, the permeation of the dominant, bigger N_2 (3.6 Å) molecules may retard the permeation of minority, smaller H_2 (2.9 Å) molecules in aged PIM-1. Thus, more N_2 molecules permeate across the membrane, resulting in lower H_2 concentration in the permeate stream and smaller H_2/N_2 selectivities. As the N_2 concentration is reduced to 30 %, H_2 being the majority gas, will preferentially permeate across aged PIM-1 membranes, owing to less competition posed by fewer N_2 molecules. With aged PIM-1/PAF-1 membranes, H_2 concentration is increased with all gas mixtures, in fact, almost 100 % of H_2 is recovered from a 30:70 mixture of N_2 and H_2, enabling room temperature H_2 recovery.

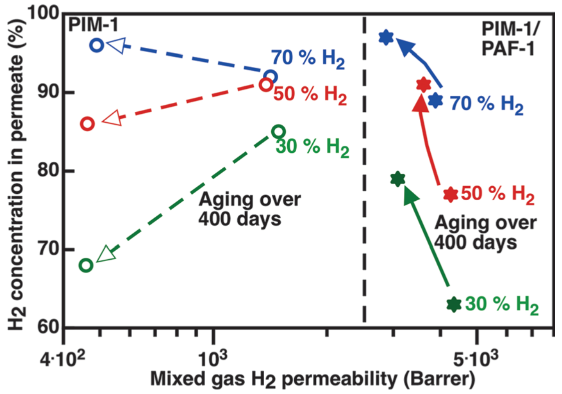

Figure 6. H_2 concentration in permeate increases when aged PIM-1/PAF-1 membranes are used to separate H_2/N_2 mixtures containing 30 to 70 vol % H_2. Arrows indicate 400 days of aging.

In summary, a remarkable form of intimate mixing between super-glassy polymers and ultraporous additive particles has been uncovered. The attractive surface chemistry of PAF-1 combined with its extreme porosity allows for intercalation of the side chains of PIM-1, which tailor the porosity of the polymer over time. Small pores are propped open whereas larger ones collapse with age. This situation has been exploited to prepare a membrane that ages selectively and actually improves with time; the larger N_2 molecules are unable to cross the membrane whereas the smaller H_2 is uninhibited. H_2 can then be recovered from mixtures with N_2, an important feature in the potential use of ammonia as a H_2 storage medium.

Received: November 3, 2014

Keywords: gas separation · membranes · physical aging · polymers · porous aromatic frameworks

[1] J. Kurchan, *Nature* **2005**, *433*, 222.
[2] B. W. Rowe, S. J. Pas, A. J. Hill, R. Suzuki, B. D. Freeman, D. R. Paul, *Polymer* **2009**, *50*, 6149.
[3] a) A. F. Bushell, M. P. Attfield, C. R. Mason, P. M. Budd, Y. Yampolskii, L. Starannikova, A. Rebrov, F. Bazzarelli, P. Bernardo, J. Carolus Jansen, M. Lanč, K. Friess, V. Shantarovich, V. Gustov, V. Isaeva, *J. Membr. Sci.* **2013**, *427*, 48; b) N. B. McKeown, *ISRN Mater. Sci.* **2012**, *2012*, 513986.
[4] a) M. D. Guiver, Y. M. Lee, *Science* **2013**, *339*, 284; b) P. M. budd, B. S. Ghanem, S. Makhseed, N. B. McKeown, K. J. Msayib, C. E. Tattershall, *Chem. Commun.* **2004**, 230; c) P. M. Budd, E. S. Elabas, B. S. Ghanem, S. Makhseed, N. B. McKeown, K. J. Msayib, C. E. Tattersall, D. Wang, *Adv. Mater.* **2004**, *16*, 456.
[5] F. Y. Li, Y. Xiao, T.-S. Chung, S. Kawi, *Macromolecules* **2012**, *45*, 1427.
[6] L. M. Robeson, *J. Membr. Sci.* **2008**, *320*, 390.
[7] a) B. Kim, D. Henkensmeier, H. J. Kim, J. Jang, S. Nam, T.-H. Lim, *Macromol. Res.* **2014**, *22*, 92; b) Q. Song, S. Cao, P. Zavala-Rivera, L. Ping Lu, W. Li, Y. Ji, S. A. Al-Muhtaseb, A. K. Cheetham, E. Sivaniah, *Nat. Commun.* **2013**, *4*, 1918.
[8] Q. Song, S. Cao, R. H. Pritchard, B. Ghalei, S. A. Al-Muhtaseb, E. M. Terentjev, A. K. Cheetham, E. Sivaniah, *Nat. Commun.* **2014**, *5*, 4813.
[9] a) J. Ahn, W.-J. Chung, I. Pinnau, J. Song, N. Du, G. P. Robertson, M. D. Guiver, *J. Membr. Sci.* **2010**, *346*, 280; b) S. J. D. Smith, B. P. Ladewig, A. J. Hill, C. H. Lau, M. R. H. Hill, *Scientific Reports*, **2014**, doi: 10.1038/srep07823.
[10] Q. Song, S. K. Nataraj, M. V. Roussenova, J. C. Tan, D. J. Hughes, W. Li, P. Bourgoin, M. A. Alam, A. K. Cheetham, S. A. Al-Muhtaseb, E. Sivaniah, *Energy Environ. Sci.* **2012**, *5*, 8359.
[11] W. I. F. David, J. W. Makepeace, S. K. Callear, H. M. A. Hunter, J. D. Taylor, T. J. Wood, M. O. Jones, *J. Am. Chem. Soc.* **2014**, *136*, 13082.
[12] G. Q. Lu, J. C. Diniz da Costa, M. Duke, S. Giessler, R. Socolow, R. H. Williams, T. Kreutz, *J. Colloid Interface Sci.* **2007**, *314*, 589.
[13] R. W. Baker, *Ind. Eng. Chem. Res.* **2002**, *41*, 1393.
[14] B. S. Ghanem, R. Swaidan, X. Ma, E. Litwiller, I. Pinnau, *Adv. Mater.* **2014**, *26*, 6696.
[15] M. Carta, M. Croad, R. Malpass-Evans, J. C. Jansen, P. Bernardo, G. Clarizia, K. Friess, M. Lanč, N. B. McKeown, *Adv. Mater.* **2014**, *26*, 3526.
[16] C. H. Lau, P. T. Nguyen, M. R. Hill, A. W. Thornton, K. Konstas, C. M. Doherty, R. J. Mulder, L. Bourgeois, A. C. Y. Liu, D. J. Sprouster, J. P. Sullivan, T. J. Bastow, A. J. Hill, D. L. Gin, R. D. Noble, *Angew. Chem. Int. Ed.* **2014**, *53*, 5322; *Angew. Chem.* **2014**, *126*, 5426.
[17] T. Ben, H. Ren, S. Ma, D. Cao, J. Lan, X. Jing, W. Wang, J. Xu, F. Deng, J. M. Simmons, S. Qiu, G. Zhu, *Angew. Chem. Int. Ed.* **2009**, *48*, 9457; *Angew. Chem.* **2009**, *121*, 9621.
[18] K. Konstas, J. W. Taylor, A. W. Thornton, C. M. Doherty, W. X. Lim, T. J. Bastow, D. F. Kennedy, C. D. Wood, B. J. Cox, J. M. Hill, A. J. Hill, M. R. Hill, *Angew. Chem. Int. Ed.* **2012**, *51*, 6639; *Angew. Chem.* **2012**, *124*, 6743.
[19] A. F. Bushell, P. M. Budd, M. P. Attfield, J. T. A. Jones, T. Hasell, A. I. Cooper, P. Bernardo, F. Bazzarelli, G. Clarizia, J. C. Jansen, *Angew. Chem. Int. Ed.* **2013**, *52*, 1253; *Angew. Chem.* **2013**, *125*, 1291.
[20] C. L. Staiger, S. J. Pas, A. J. Hill, C. J. Cornelius, *Chem. Mater.* **2008**, *20*, 2606.
[21] T. C. Merkel, Z. He, I. Pinnau, B. D. Freeman, P. Meakin, A. J. Hill, *Macromolecules* **2003**, *36*, 6844.
[22] J. Weber, N. Du, M. D. Guiver, *Macromolecules* **2011**, *44*, 1763.
[23] S. Jain, J. G. P. Goossens, G. W. M. Peters, M. van Duin, P. J. Lemstra, *Soft Matter* **2008**, *4*, 1848.
[24] A. Tuteja, M. E. Mackay, C. J. Hawker, B. Van Horn, *Macromolecules* **2005**, *38*, 8000.
[25] M. E. Mackay, T. T. Dao, A. Tuteja, D. L. Ho, B. Van Horn, H.-C. Kim, C. J. Hawker, *Nat. Mater.* **2003**, *2*, 762.
[26] A. J. Hill, S. J. Pas, T. J. Bastow, M. I. Burgar, K. Nagai, L. G. Toy, B. D. Freeman, *J. Membr. Sci.* **2004**, *243*, 37.
[27] C. R. Mason, M. G. Buonomenna, G. Golemme, P. M. Budd, F. Galiano, A. Figoli, K. Friess, V. Hynek, *Polymer* **2013**, *54*, 2222.
[28] a) *Materials Science of Membranes for Gas and Vapor Separation*, Wiley, Chichester, **2006**.